Electronic Supplementary Material (ESI) for Physical Chemistry Chemical Physics.

Supplementary information

Optoelectronic Simulation of Four-terminal All-inorganic $CsPbI_3$/CZTSSe Tandem Solar Cell with High Power Conversion Efficiency

Dan Wang[1], Shunwei Yao[1], Yening Zhong[1], Lin Peng[1*], Tingting Shi[2], Jin Chen[1,3], Xiaolin Liu[1], Jia Lin[1*]

[1]Department of Physics, Shanghai University of Electric Power, Shanghai 200090, China

[2]Department of Physics, Jinan University, Guangzhou 510632, China

[3]Department of Electronic Engineering, Shanghai Jiao Tong University, Shanghai 200240, China

*Corresponding author. Lin Peng, Email: plpeng@shiep.edu.cn

Jia Lin, Email: jlin@shiep.edu.cn

COMSOL Multiphysics simulation package has been used for simulation of perovskite and CZTSSe thin-film solar cells. In this study, the comprehensive simulations of the 4T tandem solar cell have to deal with the electromagnetic and carrier transport behaviors. Although the top PSC and bottom CZTSSe cell are electrically independent, the cells are optically coupled, so that the light transmits through the top cell and then reaches the bottom cell. Although the thermodynamic response has to be included to better mimic the device operation in some circumstances, the photoelectric simulation is sufficient for the considered 4T tandem solar cell under one solar illumination. In this simulation, the input power of the plane wave with normal incident angle is used. Non-polarized sunlight incidence under standard AM1.5 spectra is introduced as the light source and the cell is assumed to be operating at room temperature. Computation methodology including optical and electrical equations are as follows. First, the Maxwell's equation (1) is solved to obtain the detailed electrical and magnetic field spatial distributions to evaluate the optical absorption:

$$\nabla \times (\nabla \times \boldsymbol{E}) - \boldsymbol{k}_0^2 \boldsymbol{\varepsilon}_r \boldsymbol{E} = 0 \qquad (1)$$

where $\boldsymbol{E}$ is the electric field, $\boldsymbol{k}_0$ is the wave-vector of incident light, and $\boldsymbol{\varepsilon}_r$ is relative permittivity. The photo-generation rate can be calculated by equation (2):

$$\boldsymbol{G}_{\boldsymbol{photo}}(\boldsymbol{\lambda}) = \frac{\boldsymbol{\varepsilon}''|\boldsymbol{E}|}{\boldsymbol{2h}} \qquad (2)$$

where $\boldsymbol{h}$ is Planck's constant and $\boldsymbol{\varepsilon}''$ is the imaginary part of $\boldsymbol{\varepsilon}_r$, which is a function of wavelength in the equation: $\boldsymbol{\varepsilon}_r(\boldsymbol{\lambda}) = (\boldsymbol{n}(\boldsymbol{\lambda}) - \boldsymbol{ik}(\boldsymbol{\lambda}))^{\boldsymbol{2}}$. Therefore, the total photo-generation rate (G_{tot}) is calculated by integration the $\boldsymbol{G}_{\boldsymbol{photo}}(\boldsymbol{\lambda})$ shown as

$\boldsymbol{G_{tot}(\lambda) = \int_{\lambda_{min}}^{\lambda_{max}} G_{photo}(\lambda) d\lambda}$ over the given wavelength range from 300 to 1200 nm. Also, it can be obtained from the built-in $\boldsymbol{S}$-parameters, which is expressed as $1 - (|S_{11}|^2 + |S_{21}|^2)$, where $|S_{11}|$ is transmission and $|S_{21}|$ is reflection in 4T solar cell device. Further, the Poisson and continuity equations (equations (3-5)) are solved in the simulation to evaluate the current density-voltage (*J-V*) characteristics of solar cells:

$$\boldsymbol{\nabla \cdot (\varepsilon_0 \cdot \varepsilon_r \nabla \emptyset) = -\rho} \quad (3)$$

$$\boldsymbol{\frac{\partial n}{\partial t} = \frac{1}{q} \nabla j_n - U_n + G_n} \quad (4)$$

$$\boldsymbol{\frac{\partial p}{\partial t} = \frac{1}{q} \nabla j_p - U_p + G_p} \quad (5)$$

where $\emptyset$ is electrostatic potential, $\boldsymbol{\rho}$ is charge density given by equation (6), $\boldsymbol{q}$ is electron charge, $\boldsymbol{\varepsilon_0}$ is the vacuum permittivity, and both the $\boldsymbol{G_n}$ and $\boldsymbol{G_p}$ are total photo-generation rate in the optical simulation $(\boldsymbol{G_n = G_p = G_{tot}})$.

$$\boldsymbol{\rho = q(n - p + N_A - N_D)} \quad (6)$$

where $\boldsymbol{n}$ and $\boldsymbol{p}$ are electron and hole concentrations, respectively. $\boldsymbol{N_A}$ and $\boldsymbol{N_D}$ are acceptor and donor density respectively. $\boldsymbol{J_n}$ and $\boldsymbol{J_p}$ are current density of electron and hole, which is expressed by electron and hole drift-diffusion as follows:

$$\boldsymbol{J_n = -q\mu_n n \nabla \emptyset + qD_n \nabla n} \quad (7)$$

$$\boldsymbol{J_p = -q\mu_p p \nabla \emptyset - qD_p \nabla p} \quad (8)$$

The key material parameters used in the electrical simulation are listed in Table 1. Here, $\boldsymbol{N_C}$ and $\boldsymbol{N_V}$ are effective density of states for electron and hole, respectively, $\boldsymbol{\mu_n}$ and $\boldsymbol{\mu_p}$ are mobility of electron and hole, respectively, $\boldsymbol{\chi}$ is electron affinity, and $\boldsymbol{E_g}$ is energy band gap. Moreover, Shockley-Read-Hall (SRH) recombination is considered as the recombination model in our simulations that is calculated by equation (9) because it has been proved as the dominant recombination mechanism in PSCs and the interfaces are treated as ideal ohmic contact in our simulations.

$$\boldsymbol{R_{SRH}} = \frac{\boldsymbol{np - n_i^2}}{\boldsymbol{\tau_p(n+n_1)+\tau_n(p+p_1)}} \qquad (9)$$

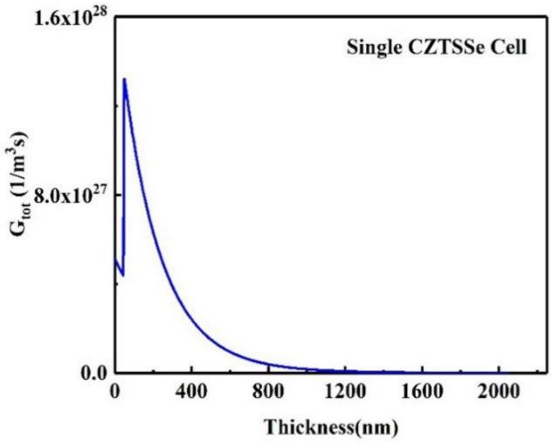

Fig. S1. G_{tot} of single CZTSSe solar cell.

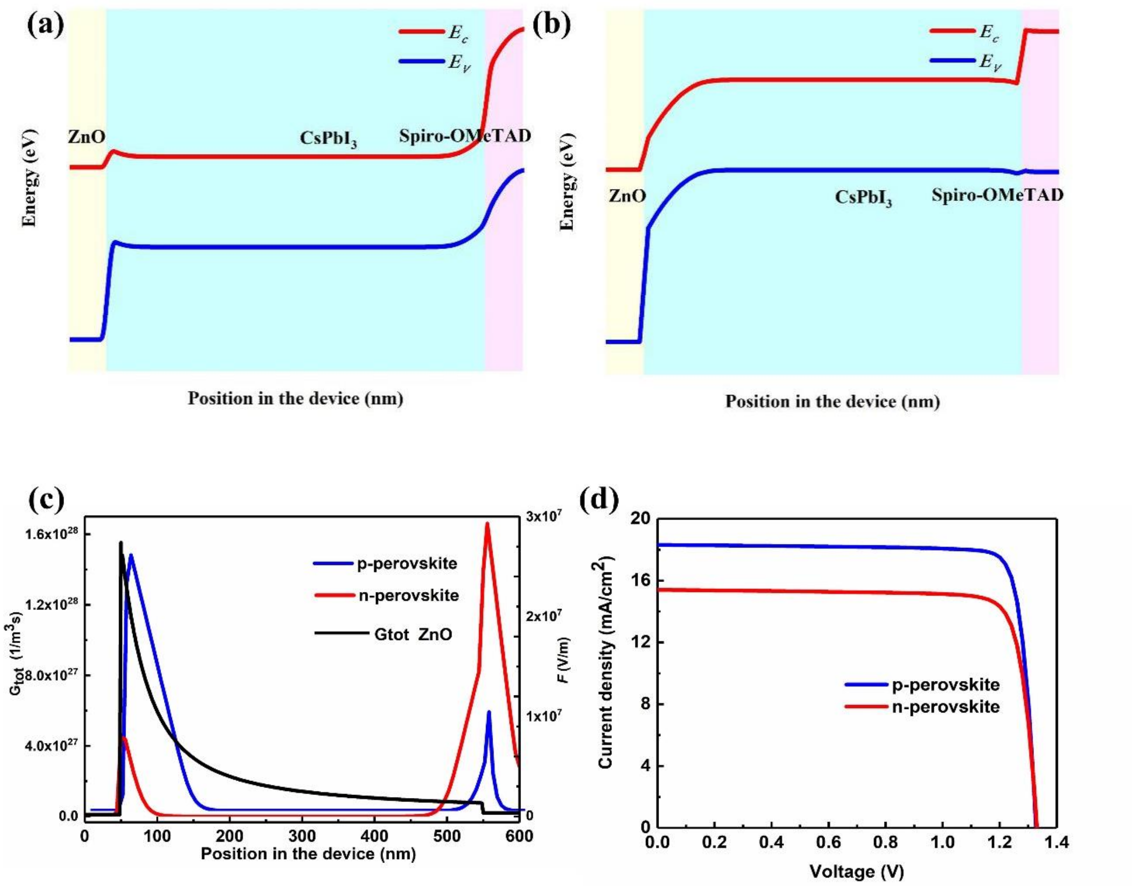

Fig. S2. Energy band-bending for top PSC of (a) n-type doped and (b) p-type doped $CsPbI_3$. (c) G_{tot} (black curve) and built-in electric field, (d) *J*-*V* curve of p-type (blue curve) and n-type (red curve) doped perovskite for top PSC.

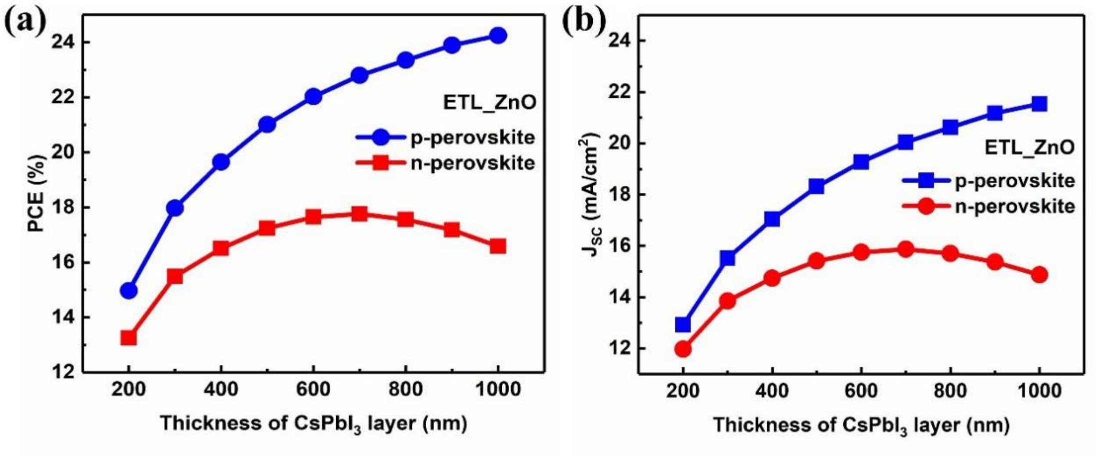

Fig. S3. (a) PCE and (b) J_{SC} of p-type (blue curve) and n-type (red curve) doped perovskite versus different thickness of $CsPbI_3$ layer for top PSC.

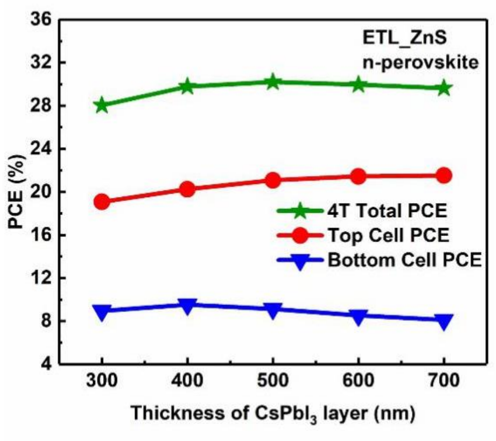

Fig. S4. 4T total PCE, top cell PCE and bottom cell PCE of n-type doped $CsPbI_3$ versus thicknesses when ZnS as electron transport layer.

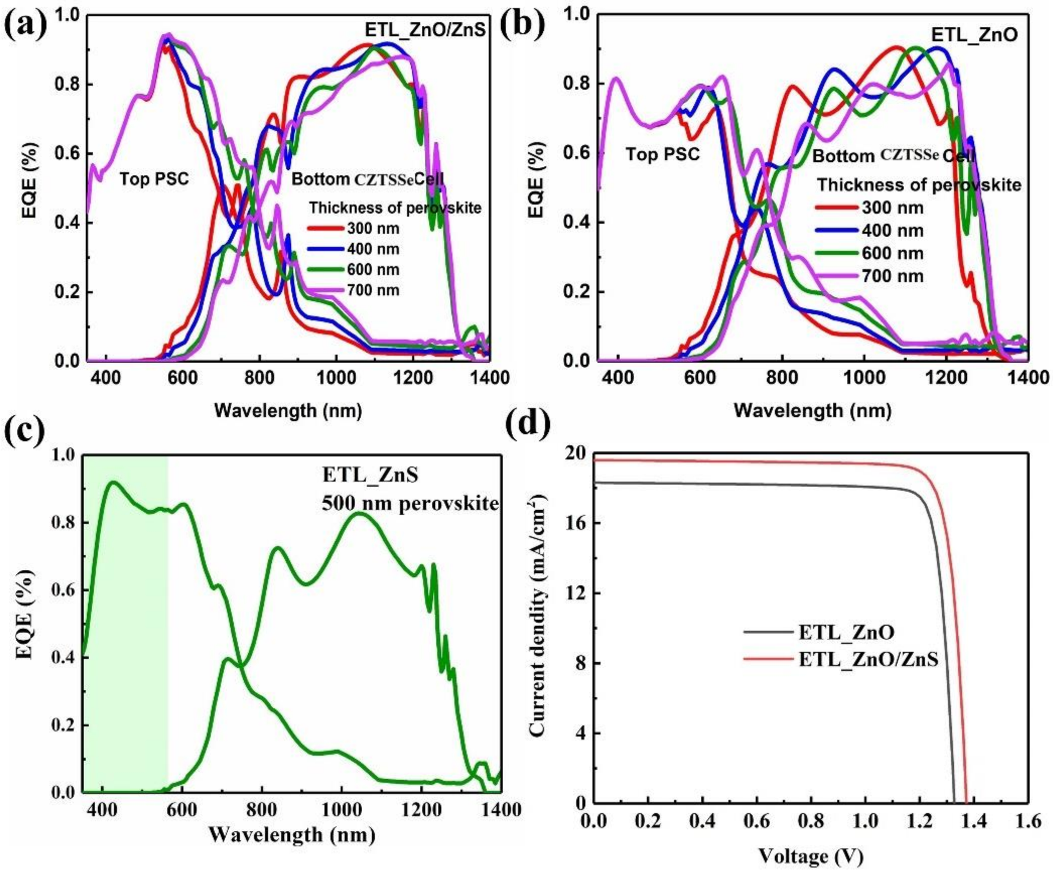

Fig. S5. (a), (b) EQE of subcells versus different thickness of $CsPbI_3$ with ZnO and ZnO/ZnS electron transport layers. (c) ZnS as ETL, 500 nm perovskite. (d) *J-V* curves with ZnO and ZnO/ZnS.

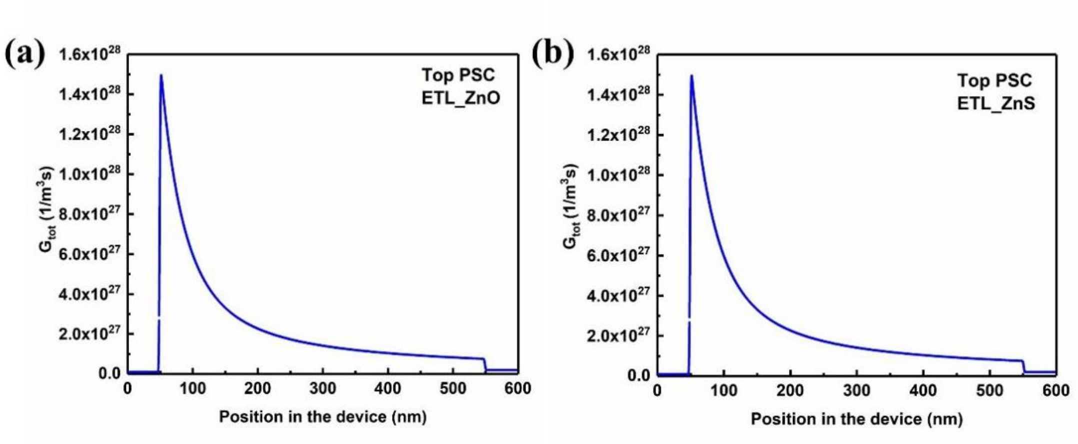

Fig. S6. G_{tot} of single CZTSSe solar cell and top PSC with (a) ZnO, (b) ZnS.

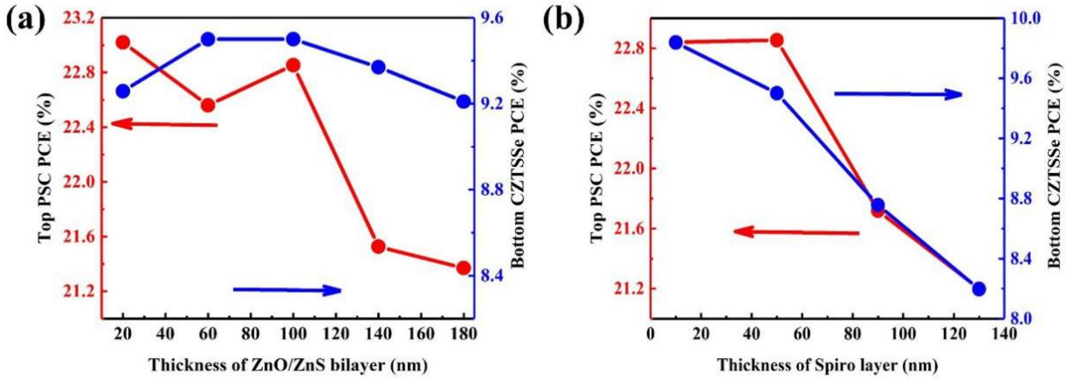

Fig. S7. PCE of top PSC and bottom CZTSSe subcell. (a) different thickness of ZnO/ZnS bilayer, (b) different thickness of Spiro layer.

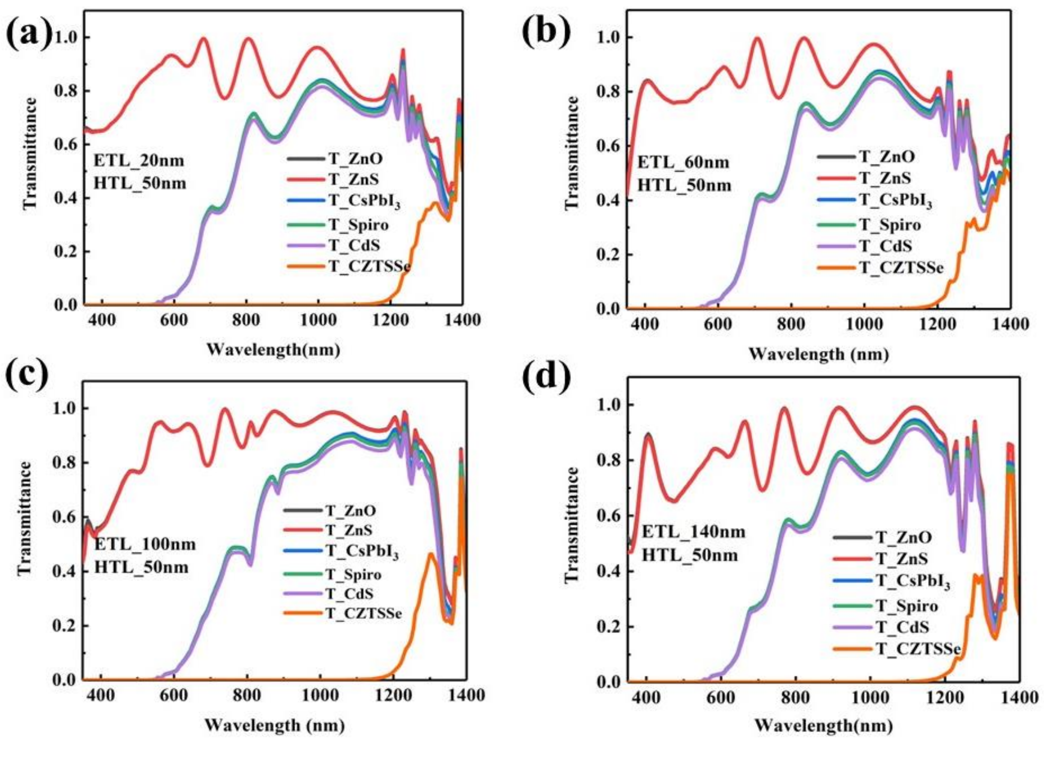

Fig. S8. Transmittance spectra of the samples with different thickness of electron transport layer when the thickness of HTL(Spiro) is 50nm, (a) 20nm, (b) 60nm, (c) 100nm, and (d) 140nm respectively.

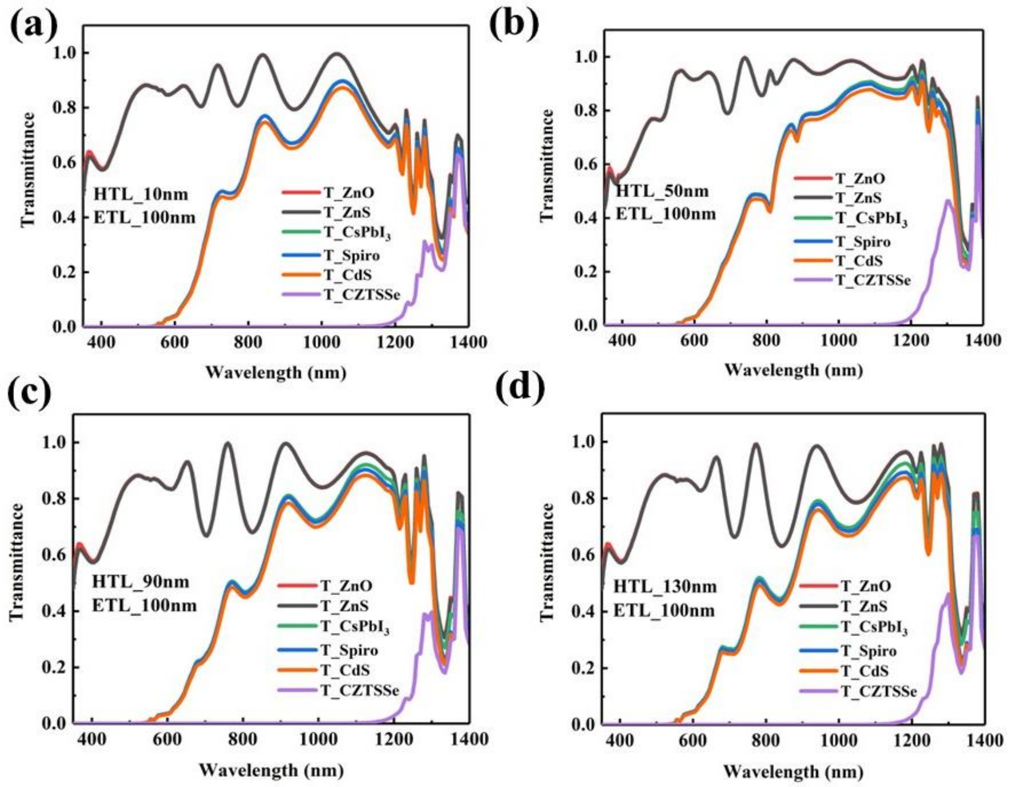

Fig. S9. Transmittance spectra of the samples with different thickness of hole transport layer when the thickness of ETL is 100nm, (a) 10nm, (b)50nm, (c) 90nm, and (d) 130nm respectively.

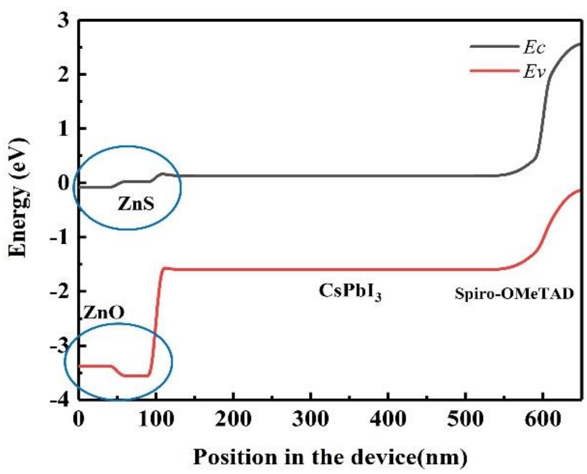

Fig. S10. Energy band-bending of materials in top PSC.

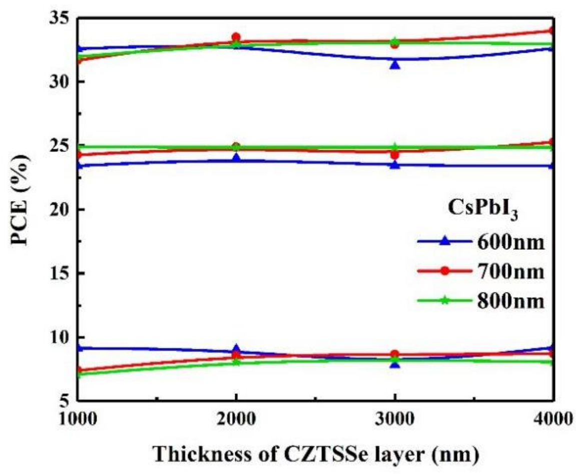

Fig. S11. PCE versus the thickness of $CsPbI_3$ and CZTSSe for 4T tandem solar cell and subcells.

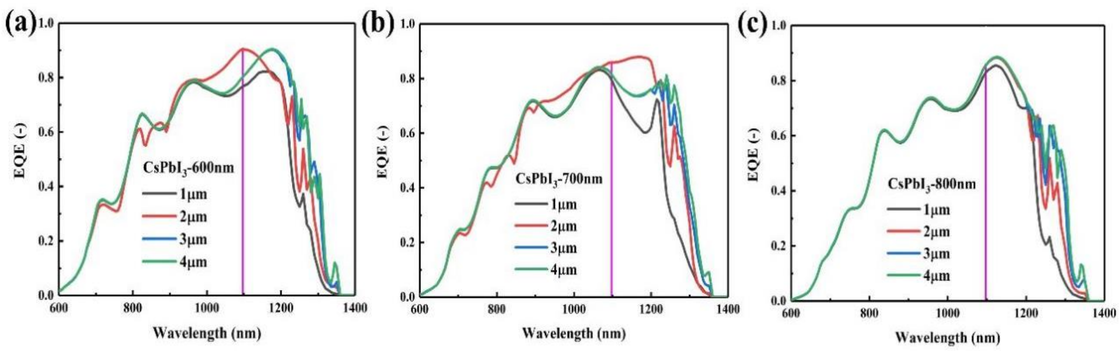

Fig. S12. EQE of subcells versus different thickness of $CsPbI_3$ and CZTSSe layer. In three cases, the thickness of CZTSSe is 1μm, 2μm, 3μm, 4μm. (a) $CsPbI_3$ is 600nm, (b) $CsPbI_3$ is 700nm, (c) $CsPbI_3$ is 800nm.

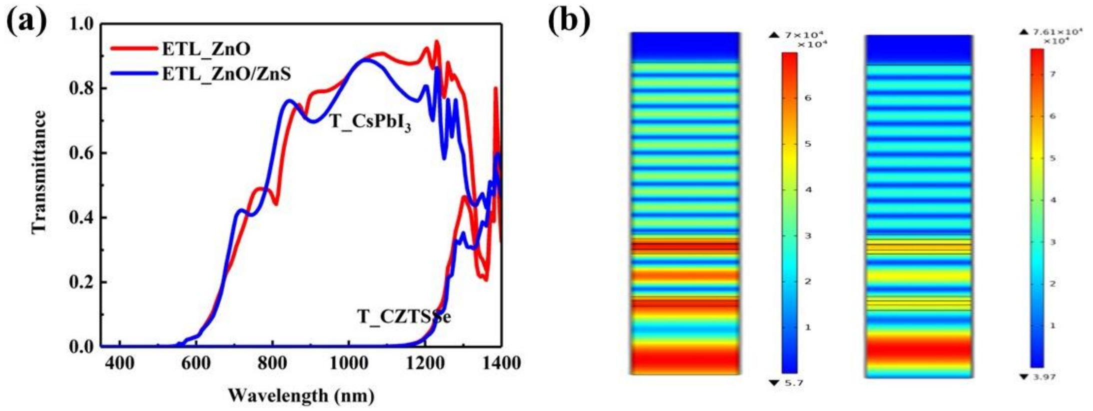

Fig. S13. (a) Transmittance spectra of the $CsPbI_3$ and CZTSSe with different ETL. (b) Colored mapping of simulated optical transmission as a function of the depth of device, and the ETL from left to right is ZnO and ZnO/ZnS, respectively.

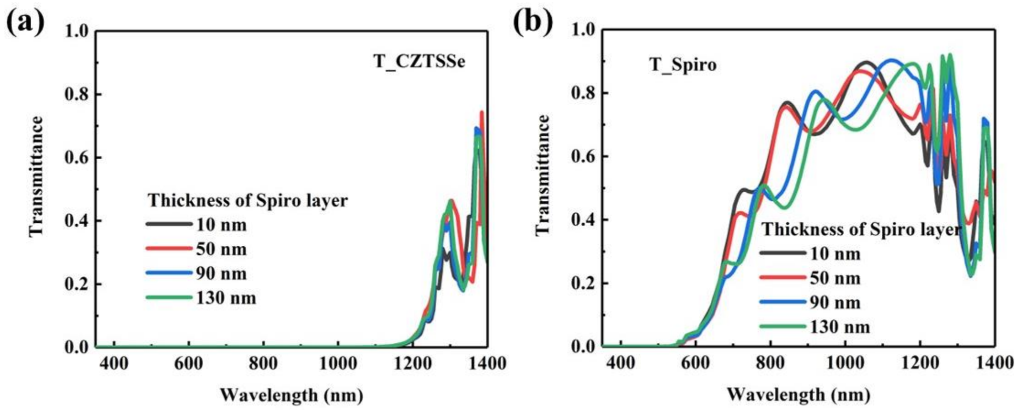

Fig. S14. Transmittance spectra with different thickness of HTL. (a) CZTSSe, (b) Spiro.

Table S1 Parameters of subcells and 4T tandem solar cell under different ZnO/ZnS thickness condition.

ZnO/ZnS thickness (nm)	Configuration	Voc (V)	Jsc (mA/cm^2)	FF	PCE (%)
20	Top PSC	1.36	19.75	0.86	23.02
	Bottom CZTSSe solar cell	0.70	15.38	0.86	9.26
	4T tandem solar cell	-	-	-	32.28
60	Top PSC	1.36	19.33	0.86	22.56
	Bottom CZTSSe solar cell	0.7	15.75	0.86	9.50
	4T tandem solar cell	-	-	-	32.06
100	Top PSC	1.36	19.59	0.86	22.85
	Bottom CZTSSe solar cell	0.70	15.75	0.86	9.50
	4T tandem solar cell	-	-	-	32.35
140	Top PSC	1.36	18.47	0.86	21.53
	Bottom CZTSSe solar cell	0.70	15.55	0.86	9.37
	4T tandem solar cell	-	-	-	30.90
180	Top PSC	1.36	18.33	0.85	21.37
	Bottom CZTSSe solar cell	0.70	15.30	0.86	9.21
	4T tandem solar cell	-	-	-	30.58

Table S2 Parameters of subcells and 4T tandem solar cell under different Spiro-OMeTAD thickness condition.

Spiro-OMeTAD thickness (nm)	Configuration	Voc (V)	Jsc (mA/cm^2)	FF	PCE (%)
	Top PSC	1.36	19.26	0.87	22.84
10	Bottom CZTSSe solar cell	0.70	16.29	0.86	9.84
	4T tandem solar cell	-	-	-	32.68
	Top PSC	1.36	19.59	0.86	22.85
50	Bottom CZTSSe solar cell	0.7	15.75	0.86	9.50
	4T tandem solar cell	-	-	-	32.35
	Top PSC	1.36	18.97	0.84	21.72
90	Bottom CZTSSe solar cell	0.70	14.59	0.86	8.76
	4T tandem solar cell	-	-	-	30.48
	Top PSC	1.36	18.87	0.83	21.72
130	Bottom CZTSSe solar cell	0.70	13.71	0.85	8.20
	4T tandem solar cell	-	-	-	29.40

Table S3 Parameters of subcells and 4T tandem solar cell under different CZTSSe thickness condition. Thickness of $CsPbI_3$ is 600nm.

CZTSSe thickness (nm)	Configuration	Voc (V)	Jsc (mA/cm^2)	FF	PCE (%)
1000	Top PSC	1.36	20.15	0.85	23.43
	Bottom CZTSSe solar cell	0.70	15.16	0.86	9.03
	4T tandem solar cell	-	-	-	32.58
2000	Top PSC	1.36	20.63	0.85	23.99
	Bottom CZTSSe solar cell	0.7	15.01	0.86	9.03
	4T tandem solar cell	-	-	-	33.03
3000	Top PSC	1.36	20.14	0.85	23.42
	4T tandem solar cell	0.70	13.48	0.83	7.84
	Bottom CZTSSe solar cell	-	-	-	31.26
4000	Top PSC	1.36	20.14	0.85	23.42
	Bottom CZTSSe solar cell	0.70	15.24	0.86	9.20
	4T tandem solar cell	-	-	-	32.62

Table S4 Parameters of subcells and 4T tandem solar cell under different CZTSSe thickness condition. Thickness of $CsPbI_3$ is 700nm.

CZTSSe thickness (nm)	**Configuration**	**Voc (V)**	**Jsc (mA/cm²)**	**FF**	**PCE (%)**
1000	Top PSC	1.36	20.93	0.85	24.28
	Bottom CZTSSe solar cell	0.70	12.75	0.83	7.41
	4T tandem solar cell	-	-	-	31.68
2000	Top PSC	1.36	21.47	0.85	24.90
	Bottom CZTSSe solar cell	0.7	14.31	0.86	8.58
	4T tandem solar cell	-	-	-	33.49
3000	Top PSC	1.36	20.93	0.85	24.27
	4T tandem solar cell	0.70	14.39	0.86	8.66
	Bottom CZTSSe solar cell	-	-	-	32.93
4000	Top PSC	1.36	21.77	0.85	25.28
	Bottom CZTSSe solar cell	0.70	14.47	0.86	8.71
	4T tandem solar cell	-	-	-	33.99

Table S5 Parameters of subcells and 4T tandem solar cell under different CZTSSe thickness condition. Thickness of $CsPbI_3$ is 800nm.

CZTSSe thickness (nm)	Configuration	Voc (V)	Jsc (mA/cm^2)	FF	PCE (%)
1000	Top PSC	1.36	21.52	0.85	24.88
	Bottom CZTSSe solar cell	0.70	12.21	0.83	7.09
	4T tandem solar cell	-	-	-	31.97
2000	Top PSC	1.36	21.51	0.85	24.88
	Bottom CZTSSe solar cell	0.7	13.51	0.85	8.07
	4T tandem solar cell	-	-	-	32.95
3000	Top PSC	1.36	21.50	0.85	24.87
	4T tandem solar cell	0.70	13.74	0.86	8.24
	Bottom CZTSSe solar cell	-	-	-	33.11
4000	Top PSC	1.36	21.51	0.85	24.88
	Bottom CZTSSe solar cell	0.70	13.51	0.85	8.07
	4T tandem solar cell	-	-	-	32.95